Risk-Aware Reserve Optimization for Power Systems Under Extreme Weather Events

Luo Xu
Department of Civil and Environmental Engineering
Princeton University
Princeton, NJ, USA
luoxu@princeton.edu

Hongtai Zeng
Department of Engineering Science
University of Oxford
Oxford, UK
hongtai.zeng@eng.ox.ac.uk

Ning Lin
Department of Civil and Environmental Engineering
Princeton University
Princeton, NJ, USA
nlin@princeton.edu

H. Vincent Poor
Department of Electrical and Computer Engineering
Princeton University
Princeton, NJ, USA
poor@princeton.edu

***Abstract*—Extreme weather events, intensified by climate change, pose increasing threats to power system reliability by introducing large uncertainties on both supply and demand sides. However, most existing studies focus on reserve optimization under normal operating conditions, where uncertainties are relatively small, and reserves are typically set using fixed margins or predefined reliability standards. Such approaches are insufficient to capture enlarged risks during evolving hazards. This paper develops a risk-aware reserve optimization framework that explicitly accounts for uncertainties from demand loss and generator contingencies. By integrating an Entropic Value-at-Risk (EVaR)-based demand risk assessment with a scenario-based generation outage model, the framework enables adaptive optimization of upward and downward reserves under evolving hazard conditions. A case study on the Puerto Rico power grid during Hurricane Fiona shows that traditional fixed-margin methods substantially underestimate reserve requirements. The proposed method provides a robust tool for enhancing power and energy system resilience under extreme events.**

***Index Terms*—reserve optimization, extreme events, uncertainty, power systems, resilience**

I. Introduction

Climate change is intensifying extreme weather events, such as tropical cyclones, heatwaves, and floodings, that increasingly disrupt electric power systems. Since the early 21st century, over 80% major U.S. blackouts were caused by weather events [1]. Hurricanes have caused two system-wide catastrophic blackouts in Puerto Rico and widespread power outages along the U.S. Gulf and East coasts [2]. In China, both the frequency and duration of power outages have risen during extreme events such as heatwaves [3].

Extreme weather events not only cause physical damage to power infrastructure but also pose significant challenges to system operation, introducing far greater uncertainty than under normal steady-state conditions [4]. Also, extreme events such as hurricanes can damage distribution lines and poles, leading to widespread feeder outages in distribution networks. During such events, the demand uncertainty increases significantly [5]. On the other hand, the large-scale integration of renewable energy sources such as solar and wind has made power generation more sensitive to environmental conditions [6]. Hurricanes can damage renewable energy infrastructure and cause a sharp drop in generation output, due both to high wind speeds exceeding turbine cut-out thresholds and to large cloud structures that significantly reduce solar irradiance. These uncertainties from both the supply and demand sides collectively amplify variability in the power system's supply-demand balance, increasing short-term flexibility requirements. In particular, the simultaneous loss of generation and the surge in demand fluctuations during extreme events can rapidly exhaust available reserves and ramping capabilities. Therefore, it is critical to quantitatively assess how much flexible reserve capacity the power system must maintain under extreme weather conditions to ensure resilient operation.

However, in existing studies on resilient power system operation under extreme weather conditions, reserve capacity requirements are often set as a fixed proportion of baseline demand and imposed as constraints in optimization models [7], [8], rather than being fully optimized by accounting for system uncertainties. For example, in a risk-aware unit commitment (UC) model [8], upward reserve requirements are chosen based on North American Electric Reliability Corporation (NERC) guidelines, which specify a reference reserve margin of 15% [9]. In addition, many existing studies focus on optimizing system reserves under normal operating conditions, accounting for relatively small disturbances such as N-1 contingency [10] and common renewable generation fluctuations [11]. However, for the resilient operation of power systems during extreme weather events, reserve capacity optimization requires the

This work was supported by US National Science Foundation grant number 2103754 (as part of the Megalopolitan Coastal Transformation Hub) and a grant from the Fund for Energy Research with Corporate Partners of Princeton's Andlinger Center for Energy and the Environment. *(Luo Xu and Hongtai Zeng are co-first authors) (Corresponding author: Luo Xu).*

979-8-3315-8138-1

consideration and management of the enlarged uncertainties arising from both the supply and demand sides across the grid.

To address these gaps, this paper develops a risk-aware reserve co-optimization framework for power systems under extreme weather events. The proposed model jointly captures supply-demand uncertainties from distribution feeder failures and generator contingencies. By integrating Entropic Value-at-Risk(EVaR)-based demand uncertainty assessment with a scenario-based generation outage model, the framework enables adaptive reserve allocation that dynamically responds to evolving hazard conditions. We apply the model to Puerto Rico power grid during Hurricane Fiona, demonstrating how the framework optimize the upward and downward reserve requirements. Our results show that traditional fixed reserve margins can largely underestimate reserve requirements under extreme weather events, highlighting the importance of more precise reserve optimization using this framework.

The remainder of this paper is organized as follows. Section II presents the proposed supply–demand risk assessment and further develops the risk-aware reserve optimization model. Section III describes the case study setup and discusses the simulation results. Section IV concludes the paper and highlights potential directions for future research.

II. Risk-Aware Reserve Optimization

During extreme events such as tropical cyclones, distribution feeders are highly susceptible to faults caused by high winds, flooding, or overheating, potentially leading to widespread load disconnections. Furthermore, generator outages can significantly increase system uncertainty and operational stress. To ensure reliable system operation under extreme weather conditions, we extend the reserve assessment framework to jointly model probabilistic distribution feeder failures and N-1 generator contingencies.

Let the net demand on distribution feeder i be denoted by D_i, and its failure probability during extreme events by p_i. The expected net demand $\bar{D}_i$ on feeder i is then given by $(1-p_i)D_i$, which we adopt as the base-case operating point for subsequent analysis. During extreme events, the stochastic nature of distribution feeder outages introduces significant uncertainty, leading to deviations of the actual net demand from its expected value. The net demand deviation for feeder i, denoted by $\Delta\tilde{D}_i$, is expressed as follows:

$$\Delta\tilde{D}_i = \begin{cases} p_i D_i & \tilde{I}_i = 1 \\ -(1-p_i)D_i & \tilde{I}_i = 0 \end{cases} \tag{1}$$

where $\tilde{I}_i$ is a binary random variable indicating the operational status of the distribution feeder i, and $\tilde{I}_i = 1$ means the feeder is intact.

To quantify the risks associated with distribution feeder failures, we adopt the Entropic Value-at-Risk (EVaR) [12] as the primary risk measure. Compared to traditional methods based on Conditional Value-at-Risk (CVaR) [13], which typically rely on the sample average approximation approach and can become computationally burdensome, EVaR offers superior tractability in handling large numbers of discrete random variables and significantly reduces computational complexity. Therefore, we use $\text{EVaR}_{1-\alpha}(\sum_{i\in\mathcal{D}}\Delta\tilde{D}_i)$ and $\text{EVaR}_{1-\alpha}(-\sum_{i\in\mathcal{D}}\Delta\tilde{D}_i)$ to assess the positive and negative deviations of total net demand relative to its mean value under feeder failure uncertainty, where $1-\alpha$ is the predefined confidence level. These EVaR terms can then be used to quantify the upward and downward reserve requirements induced by distribution feeder failures. According to the definition of EVaR, we have:

$$\begin{aligned}\text{EVaR}_{1-\alpha}(\sum_{i\in\mathcal{D}}\Delta\tilde{D}_i) = \min_{s^+>0} s^+ \sum_{i\in\mathcal{D}} \ln \Bigg((1-p_i)\exp\Big(\frac{p_i D_i}{s^+}\Big) \\ + p_i \exp\Big(-\frac{(1-p_i)D_i}{s^+}\Big)\Bigg) - s^+ \ln\alpha\end{aligned} \tag{2a}$$

$$\begin{aligned}\text{EVaR}_{1-\alpha}(-\sum_{i\in\mathcal{D}}\Delta\tilde{D}_i) = \min_{s^->0} s^- \sum_{i\in\mathcal{D}} \ln \Bigg(p_i\exp\Big(\frac{(1-p_i)D_i}{s^-}\Big) \\ + (1-p_i) \exp\Big(\frac{-p_i D_i}{s^-}\Big)\Bigg) - s^- \ln\alpha\end{aligned} \tag{2b}$$

where s^+, s^- are are the reciprocals of the variables appearing in the moment-generating functions associated with EVaR terms, $\mathcal{D}$ is the set of distribution feeders.

The computation of the EVaR terms in Eq. (2) can be reformulated as a conic optimization problem by introducing additional auxiliary variables $z_i^+, z_i^-, v_i^+, v_i^-, w_i^+, w_i^-$, as shown in Eq. (3):

$$\begin{aligned}\text{EVaR}_{1-\alpha}(\sum_{i\in\mathcal{D}}\Delta\tilde{D}_i) = \min_{s^+>0, z_i^+, v_i^+, w_i^+} & \sum_{i\in\mathcal{D}} z_i^+ - s^+\ln\alpha \\ \text{s.t.} \quad (v_i^+, s^+, -(1-p_i)D_i - z_i^+) &\in \mathcal{K}_{\text{exp}}, \quad i\in\mathcal{D}, \\ (w_i^+, s^+, p_i D_i - z_i^+) &\in \mathcal{K}_{\text{exp}}, \quad i\in\mathcal{D}, \\ p_i v_i^+ + (1-p_i) w_i^+ &\le s^+, \quad i\in\mathcal{D}.\end{aligned} \tag{3a}$$

$$\begin{aligned}\text{EVaR}_{1-\alpha}(-\sum_{i\in\mathcal{D}}\Delta\tilde{D}_i) = \min_{s^->0, z_i^-, v_i^-, w_i^-} & \sum_{i\in\mathcal{D}} z_i^- - s^-\ln\alpha \\ \text{s.t.} \quad (v_i^-, s^-, (1-p_i)D_i - z_i^-) &\in \mathcal{K}_{\text{exp}}, \quad i\in\mathcal{D}, \\ (w_i^-, s^-, -p_i D_i - z_i^-) &\in \mathcal{K}_{\text{exp}}, \quad i\in\mathcal{D}, \\ p_i v_i^- + (1-p_i) w_i^- &\le s^-, \quad i\in\mathcal{D}.\end{aligned} \tag{3b}$$

where $\mathcal{K}_{\text{exp}} = \left\{(x,y,z)\in\mathbb{R}^3 \;\middle|\; y>0,\ ye^{z/y}\le x\right\}$ represents the exponential cone.

To further quantify reserve requirements under generator contingencies, a scenario-based formulation is adopted to establish the lower bounds of both upward and downward reserve capacities. Specifically, let R_g^u and R_g^d denote the upward and downward reserve capabilities provided by generator $g\in\mathcal{G}$ in the base (non-contingency) case. For each contingency set $\mathcal{C}_s\in\mathcal{C}$ ($s\in[\![|\mathcal{C}|]\!] = \{1,2,\cdots,|\mathcal{C}|\}$) where

$\mathcal{C}_s$ contains a subset of generators assumed to be out of service, the lower bound for the system-wide upward reserve, denoted as $R^{u,\text{sys}}$, must ensure sufficient upward flexibility to compensate for both the worst-case loss of upward reserves together with the associated generation loss, and the potential positive deviations in total net demand quantified by the EVaR term in (2a). The detailed formulation of $R^{u,\text{sys}}$ is provided in Eq. (4a). Similarly, the lower bound for the system-wide downward reserve, $R^{d,\text{sys}}$, must account for both the potential decreases in net demand and the worst-case loss of downward reserves together with the associated generation loss under contingency scenarios. For each generator $g \in \mathcal{C}_s$ assumed to be out of service, since the generation loss P_g actually alleviates the need for downward adjustment. This mitigating effect is therefore represented by a negative sign preceding P_g, as shown in Eq. (4b).

$$R^{u,\text{sys}} = \max_s \{ \sum_{g\in\mathcal{C}_s} (R_g^u + P_g) \} + \text{EVaR}_{1-\alpha}(\sum_{i\in\mathcal{D}} \Delta\tilde{D}_i) \quad (4a)$$

$$R^{d,\text{sys}} = \max_s \{ \sum_{g\in\mathcal{C}_s} (R_g^d - P_g) \} + \text{EVaR}_{1-\alpha}(-\sum_{i\in\mathcal{D}} \Delta\tilde{D}_i) \quad (4b)$$

Following the general contingency analysis discussed above, this study further investigates the effects of distribution feeder failures and N-1 generator contingencies on reserve requirements in risk-averse power dispatch, as shown in Eq. (5).

$$\min_{\substack{U_g, P_g, R_g^u, R_g^d, R^{\text{sys}},\\ p_s^+, p_s^-, r_{g,s}^u, r_{g,s}^d}} \sum_{g\in\mathcal{G}} C_g\big(P_g\big) + C^{\text{res}} R^{\text{sys}} + c^{\text{M}} \sum_{s\in[\![|\mathcal{C}|]\!]} (p_s^+ + p_s^-) \quad (5a)$$

$$\text{s.t.} \quad \sum_{g\in\mathcal{G}} P_g = \sum_{i\in\mathcal{D}} \bar{D}_i, \quad (5b)$$

$$U_g P_g^{\min} \le P_g \le U_g P_g^{\max}, \quad g \in \mathcal{G}, \quad (5c)$$

$$P_g + R_g^u \le U_g P_g^{\max}, \quad g \in \mathcal{G}, \quad (5d)$$

$$P_g - R_g^d \ge U_g P_g^{\min}, \quad g \in \mathcal{G}, \quad (5e)$$

$$R_g^u \le U_g R_g^{\max}, R_g^d \le U_g R_g^{\max}, \quad g \in \mathcal{G}, \quad (5f)$$

$$\sum_{g\in\mathcal{G}} R_g^u \le R^{\text{sys}}, \sum_{g\in\mathcal{G}} R_g^d \le R^{\text{sys}}, \quad (5g)$$

$$\sum_{g\in\mathcal{G}\setminus\mathcal{C}_s} (P_g + r_{g,s}^u - r_{g,s}^d) + p_s^+ - p_s^- = \sum_{i\in\mathcal{D}} \bar{D}_i, s \in [\![|\mathcal{C}|]\!], \quad (5h)$$

$$U_g P_g^{\min} \le P_g + r_{g,s}^u - r_{g,s}^d \le U_g P_g^{\max}, s \in [\![|\mathcal{C}|]\!], g \in \mathcal{G} \setminus \mathcal{C}_s, \quad (5i)$$

$$r_{g,s}^u \le R_g^u, r_{g,s}^d \le R_g^d, \quad s \in [\![|\mathcal{C}|]\!], g \in \mathcal{G} \setminus \mathcal{C}_s, \quad (5j)$$

$$\sum_{g\in\mathcal{G}} R_g^u \ge \sum_{g\in\mathcal{C}_s} (R_g^u + P_g) + \text{EVaR}_{1-\alpha}(\sum_{i\in\mathcal{D}} \Delta\tilde{D}_i), s \in [\![|\mathcal{C}|]\!], \quad (5k)$$

$$\sum_{g\in\mathcal{G}} R_g^d \ge \sum_{g\in\mathcal{C}_s} (R_g^d - P_g) + \text{EVaR}_{1-\alpha}(\sum_{i\in\mathcal{D}} -\Delta\tilde{D}_i), s \in [\![|\mathcal{C}|]\!], \quad (5l)$$

$$U_g \in \{0,1\}, R_g^u, R_g^d, R^{\text{sys}} \ge 0, \quad g \in \mathcal{G}, \quad (5m)$$

$$r_{g,s}^u, r_{g,s}^d, p_s^+, p_s^- \ge 0, \quad g \in \mathcal{G}, s \in [\![|\mathcal{C}|]\!]. \quad (5n)$$

where $\mathcal{G}, \mathcal{D}$ denote the sets of generators, distribution feeders, and generator contingencies, respectively; $\mathcal{C} = \{\emptyset\} \cup \{\{g\} | g \in \mathcal{G}\}$ denote the set of generator contingencies, including the base (non-contingency) case and all N-1 generator outage scenarios; $U_g, P_g, P_g^{\min}, P_g^{\max}, C_g(\cdot)$ represent the commitment status, the active power output, minimum output, maximum output and cost function of generator $g \in \mathcal{G}$, respectively; $\bar{D}_i$ denotes the expected net demand on distribution feeder $i \in \mathcal{D}$; R_g^u, R_g^d are the upward and downward reserve capacities provided by generator $g \in \mathcal{G}$; R^{sys} is the system-wide reserve requirement, and C^{res} is the cost coefficient for reserve procurement, p_s^+, p_s^- are slack variables representing positive and negative power imbalances (e.g., load shedding or over-generation) under the s-th contingency, with c^{M} being the cost coefficient for such imbalances; $r_{g,s}^u, r_{g,s}^d$ are the upward and downward re-dispatch adjustments of generator g under the s-th contingency.

The objective in Eq. (5) minimizes the total operational cost, including generation costs, reserve procurement costs, and the expected cost of power imbalances. Eq. (5b) enforces supply–demand balance in the base case. The generation is constrained by minimum and maximum capacity limits and unit commitment status, as defined in Eq. (5c). The ramping capability of generator g is modeled in Eqs. (5d)-(5f). The total procured system reserve R^{sys} serves as an upper bound on the sum of individual unit reserves, as expressed in Eq. (5g). Under contingency scenarios, power balance must be maintained through re-dispatch and imbalance correction. This is enforced by Eq. (5h), which requires that the re-dispatch of surviving units, along with slack variables p_s^+ and p_s^-, restores balance in each generator outage scenario s. Eqs. (5i)-(5j) ensure that re-dispatch adjustments remain within generator capacity limits and do not exceed pre-allocated upward and downward reserves. Eqs. (5k)-(5l) ensure that the total upward and downward reserves exceed their respective lower bounds when accounting for distribution failures and N-1 generator contingencies. Finally, the domain constraints for all decision variables are specified in Eqs. (5m)-(5n).

III. Case Study

Here, we use the Puerto Rico power grid following the configuration in Ref. [8], which includes a high-voltage transmission network and a distribution network with nearly 1,000 feeders, as shown in Fig. 1. The system is analyzed during Hurricane Fiona on September 18th, 2022. Similarly, we apply the physics-based wind profile model [14] to simulate the spatiotemporal wind hazard during Hurricane Fiona based on the recorded hurricane data from the International Best Track Archive for Climate Stewardship (IBTrACS) [15]. The failure probability of each distribution feeder under a given wind hazard intensity is calculated using fragility functions developed for Puerto Rico [16].

Fig. 2 illustrates the distribution of feeder failure probabilities and corresponding feeder demands across the Puerto Rico grid at the local time of 12:00 pm. Each dot represents an individual feeder, where the horizontal axis denotes its

979-8-3315-8138-1

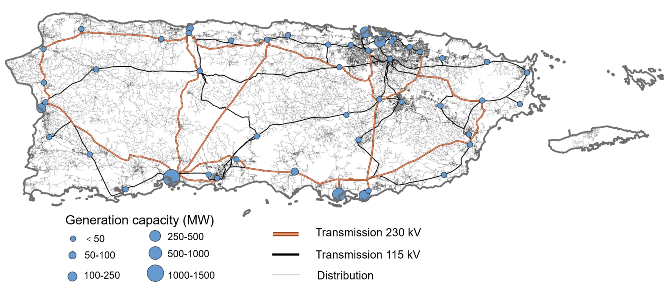

Fig. 1. Puerto Rico power grid during Hurricane Fiona in September 2022.

failure probability under the simulated wind field of Hurricane Fiona and the vertical axis indicates its feeder demand. Fig. 2 highlights the significant heterogeneity among distribution feeders in the power grid, reflecting differences in both spatial exposure and load levels. This heterogeneity represents a major contributor to the demand-side uncertainty during the extreme weather event.

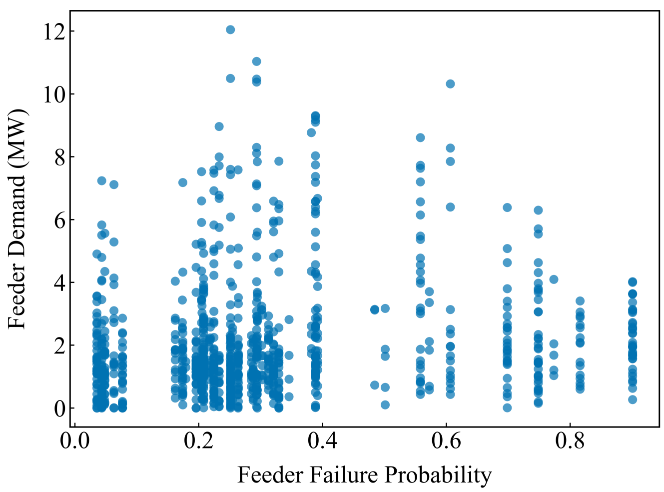

Fig. 2. Heterogeneity of distribution feeders in Puerto Rico showing failure probability during Hurricane Fiona (2022) and corresponding peak demand of each feeder.

As shown in Fig. 3, the expected net demand exhibits a declining trend under the extreme event due to the growing distribution feeder outages. However, the demand uncertainty evaluated by EVaR increases as the hazard evolves. Despite lower overall demand in the later stage, the system experiences an accumulation of risk. At the 95% confidence level, the deviation between the upper and lower EVaR bounds exceeds ±100 MW, approximately 20% of the total load, imposing greater requirements on the system's flexible reserve capacity.

As illustrated in Fig. 4, the optimized system reserves demonstrate distinct temporal variations in both upward and downward directions over the 24-hour horizon during Hurricane Fiona. Compared with the EVaR-evaluated demand-side uncertainty shown in Fig. 3, the required reserve capacities are consistently higher because the optimization jointly considers generator contingencies and distribution feeder failures. These

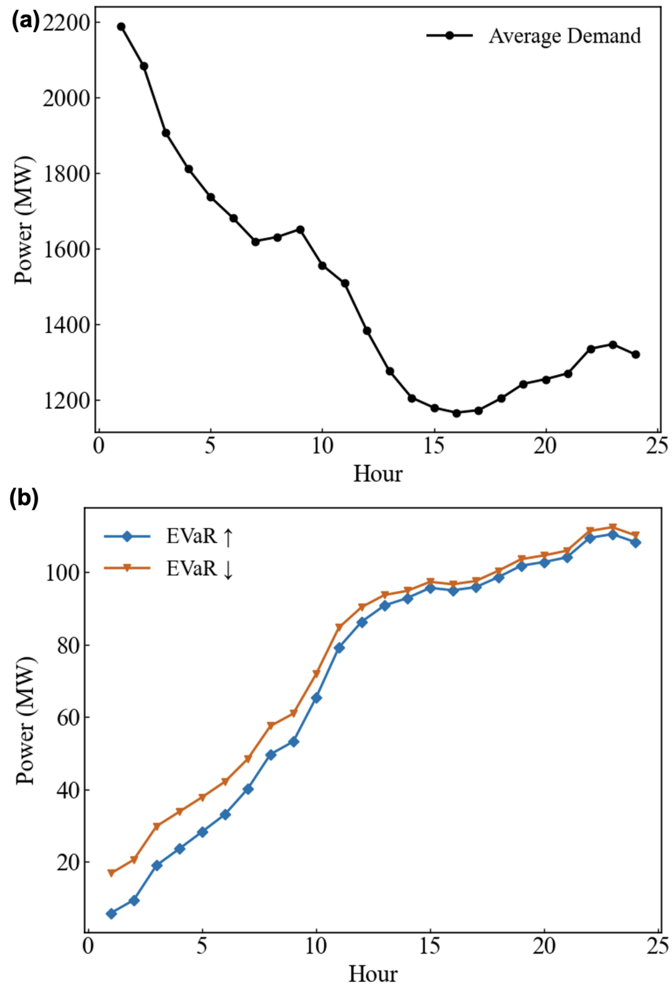

Fig. 3. Temporal evolution of system demand and uncertainty. (a) Expected net demand over 24 hours during Hurricane Fiona. (b). Upward and downward demand uncertainty represented by EVaR at a 95% confidence level.

coupled uncertainties enlarge the overall supply–demand mismatch risk, prompting the system to maintain greater flexibility.

We further compare our optimized reserves, which account for supply-demand uncertainty, with the fixed-margin method that typically sets the upward and downward reserves as 15% and 3% of total generation [17], respectively, as shown in Fig. 5. The results show that traditional fixed-margin reserves are significantly inadequate, particularly during the early stages of a hurricane when there is a rapid loss of load and high demand for downward adjustments. The fixed-margin approach underestimates the required downward reserve capacity. Moreover, as the hurricane intensifies, the system increasingly relies on upward reserves to address uncertainty arising from both demand fluctuations and generation losses.

These results also highlight that the proposed risk-aware co-optimization leads to asymmetric reserve allocation: the upward reserve remains dominant to safeguard against sudden loss of generation, while the downward reserve adapts dynamically to demand reductions. This finding confirms that the

979-8-3315-8138-1

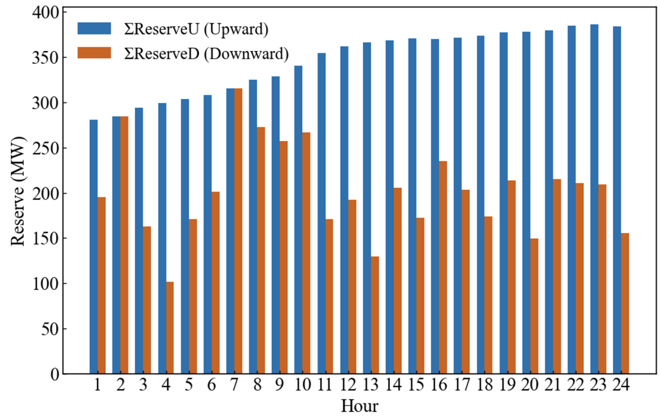

Fig. 4. Optimized system upward and downward reserves over 24 hours during Hurricane Fiona.

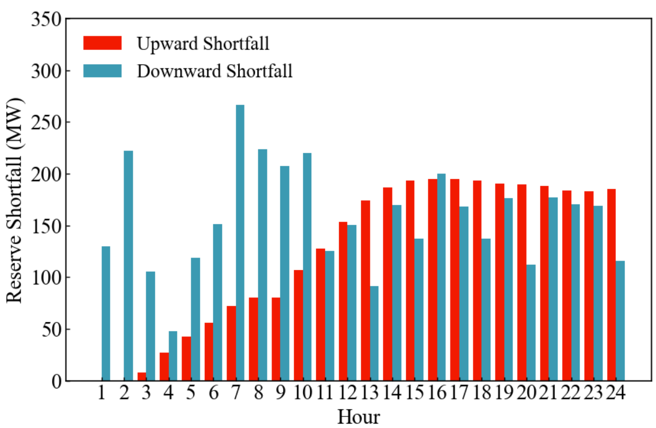

Fig. 5. Reserve shortfalls between optimized reserves and fixed-margin reserves under Hurricane Fiona.

joint supply-demand risk management framework effectively captures multi-source uncertainty and provides more robust reserve planning compared with conventional fixed-margin approaches.

IV. Conclusion

This paper has presented a risk-aware reserve optimization framework for power systems under extreme weather events. By accounting for joint supply-demand uncertainties through an EVaR-based demand loss formulation and N-1 generator contingencies, the proposed approach enables adaptive reserve allocation for both upward and downward reserve requirements under evolving natural hazards. The application to the Puerto Rico power grid under Hurricane Fiona shows that the framework effectively captures asymmetric reserve needs arising from feeder failures and generation losses. Compared with traditional fixed-margin methods, the proposed approach ensures higher system flexibility and more robust operation during extreme events. Planned future work will extend this framework to include renewable generation uncertainty and inter-temporal ramping dynamics.

References

[1] Climate Central, "Weather-related power outages rising," https://www.climatecentral.org/climate-matters/weather-related-power-outages-rising, 2024.

[2] L. Xu et al., "Resilience of renewable power systems under climate risks," *Nature Reviews Electrical Engineering*, vol. 1, no. 1, pp. 53–66, 2024.

[3] J. Liang, Y. L. Qiu, B. Wang, X. Shen, and S. Liu, "Impacts of heatwaves on electricity reliability: Evidence from power outage data in China," *Iscience*, vol. 28, no. 2, 2025.

[4] A. C. Reilly, G. L. Tonn, C. Zhai, and S. D. Guikema, "Hurricanes and power system reliability-the effects of individual decisions and system-level hardening," *Proceedings of the IEEE*, vol. 105, no. 7, pp. 1429–1442, 2017.

[5] G. Li, P. Zhang, P. B. Luh, W. Li, Z. Bie, C. Serna, and Z. Zhao, "Risk analysis for distribution systems in the northeast us under wind storms," *IEEE Transactions on Power Systems*, vol. 29, no. 2, pp. 889–898, 2013.

[6] L. Xu, N. Lin, H. V. Poor, D. Xi, and A. D. Perera, "Quantifying cascading power outages during climate extremes considering renewable energy integration," *Nature Communications*, vol. 16, no. 1, p. 2582, 2025.

[7] M. F. Anjos, A. J. Conejo *et al.*, "Unit commitment in electric energy systems," *Foundations and Trends® in Electric Energy Systems*, vol. 1, no. 4, pp. 220–310, 2017.

[8] L. Xu, H. Zeng, N. Lin, Y. Yang, Q. Guo, and H. V. Poor, "Risk-aware electricity dispatch with large-scale distributed renewable integration under climate extremes," *Proceedings of the National Academy of Sciences*, vol. 122, no. 20, p. e2426620122, 2025.

[9] North American Electric Reliability Corporation, "Summer reliability assessment," https://www.nerc.com/pa/rapa/ra/, 2013.

[10] S. A. Hosseini, M. Toulabi, A. Ashouri-Zadeh, and A. M. Ranjbar, "Modified power reserve management solution in power system considering frequency constraints," *IEEE Systems Journal*, vol. 14, no. 1, pp. 1125–1134, 2019.

[11] H. Holttinen, M. Milligan, E. Ela, N. Menemenlis, J. Dobschinski, B. Rawn, R. J. Bessa, D. Flynn, E. Gomez-Lazaro, and N. K. Detlefsen, "Methodologies to determine operating reserves due to increased wind power," *IEEE Transactions on Sustainable Energy*, vol. 3, no. 4, pp. 713–723, 2012.

[12] A. Ahmadi-Javid, "Entropic value-at-risk: A new coherent risk measure," *Journal of Optimization Theory and Applications*, vol. 155, no. 3, pp. 1105–1123, 2012.

[13] R. T. Rockafellar, S. Uryasev *et al.*, "Optimization of conditional value-at-risk," *Journal of Risk*, vol. 2, pp. 21–42, 2000.

[14] D. R. Chavas, N. Lin, and K. Emanuel, "A model for the complete radial structure of the tropical cyclone wind field. part i: Comparison with observed structure," *Journal of the Atmospheric Sciences*, vol. 72, no. 9, pp. 3647–3662, 2015.

[15] K. R. Knapp, M. C. Kruk, D. H. Levinson, H. J. Diamond, and C. J. Neumann, "The international best track archive for climate stewardship (ibtracs) unifying tropical cyclone data," *Bulletin of the American Meteorological Society*, vol. 91, no. 3, pp. 363–376, 2010.

[16] L. Xu, N. Lin, D. Xi, K. Feng, and H. V. Poor, "Hazard resistance-based spatiotemporal risk analysis for distribution network outages during hurricanes," *IEEE Transactions on Power Systems*, vol. 40, no. 3, pp. 2143–2152, 2025.

[17] K. Jiang, N. Liu, K. Wang, Y. Chen, J. Wang, and Y. Liu, "Spatiotemporal assessment of renewable adequacy during diverse extreme weather events in china," *Nature Communications*, vol. 16, no. 1, p. 5198, 2025.

979-8-3315-8138-1